Preparation and Optical Characterization of Two Photoactive Poly(bisphenol A ethoxylate diacrylate) Copolymers Containing Designed Amino-Nitro-Substituted Azobenzene Units, Obtained via Classical and Frontal Polymerization, Using Novel Ionic Liquids as Initiators

Javier Illescas,[1,2] Jesús Ortíz-Palacios,[1] Jair Esquivel-Guzmán,[1] Yessica S. Ramirez-Fuentes,[1] Ernesto Rivera,[1] Omar G. Morales-Saavedra,[3] Antonio A. Rodríguez-Rosales,[3] Valeria Alzari,[2] Daniele Nuvoli,[2] Sergio Scognamillo,[2] Alberto Mariani[2]

[1]Instituto de Investigaciones en Materiales, Universidad Nacional Autónoma de México. Circuito exterior Ciudad Universitaria C.P. 04510 México DF
[2]Dipartimento di Chimica e Farmacia, Università di Sassari, and local INSTM Unit, Via Vienna 2, 07100 Sassari, Italy
[3]Centro de Ciencias Aplicadas y Desarrollo Tecnológico, Universidad Nacional Autónoma de México. Circuito exterior Ciudad Universitaria C.P. 04510 México DF
Correspondence to: A. Mariani (E-mail: mariani@uniss.it) or E. Rivera (E-mail: riverage@iim.unam.mx)

Received 1 December 2011; accepted 25 January 2012; published online 23 February 2012
DOI: 10.1002/pola.25962

ABSTRACT: The frontal polymerization (FP) of bisphenol A ethoxylate diacrylate (BPAEDA) was carried with and without the presence of two different azobenzene comonomers by means of an external heating source. The first azomonomer (MDR-1) is a derivative of disperse red-1, *N*-ethyl-*N*-(2-hydroxyethyl)-4-(4-nitrophenylazo)aniline, whereas the second (E)-2-(4-((4-nitrophenyl)diazenyl)phenyl)-5,8,11-trioxa-2-azatridecan-13-yl methacrylate (4PEGMAN) comes from the azo-dye *N*-methyl-*N*-{4-[(E)-(4-nitrophenyl)diazenyl]phenyl}-*N*-(11-hydroxy-3,6,9-trioxaundecas-1-yl) amine. In this work, an ionic liquid trihexyltetradecylphosphonium persulfate was used as initiator. This compound produced stable propagating polymerization fronts with good velocities and moderate maximum temperature values. Moreover, this initiator prevented bubble formation and was found to be the most efficient when it was used in lower amounts with respect to other initiators, such as benzoyl peroxide, 2,2′-azobisisobutyronitrile, aliquat persulfate®, and tetrabutylphosphonium persulfate. The thermal properties of the obtained polymers and copolymers were determined by thermogravimetric analysis and differential scanning calorimetry. The nonlinear optical (NLO) characterizations of the developed BPAEDA/MDR-1 and BPAEDA/4PEGMAN copolymers were performed according to the Z-Scan technique in film samples prepared by classical polymerization. It has been proven that samples with higher 4PEGMAN content (0.26 mol %) exhibited outstanding cubic NLO-activity with positive NLO-refractive coefficients in the promising range of $n_2 = +3.2 \times 10^{-4}$ esu. © 2012 Wiley Periodicals, Inc. J Polym Sci Part A: Polym Chem 50: 1906–1916, 2012

KEYWORDS: azopolymers; frontal polymerization; initiators; NLO; radical polymerization; Z-Scan

INTRODUCTION Azopolymers have been considered as highly versatile materials, due to their light response, nonlinear optical (NLO) effects and the photoinduced motions which occur on them, when they are irradiated with polarized laser light.[1] Several reviews covering most of the implications of azobenzene in polymer structures have been published.[1–4] At the beginning, research on azobenzene molecules focused mainly on the development of dyes. However, since the discover of the trans–cis photoisomerization of azobenzene in the 1950s and its potential applications in optics, this research field has evolved significantly.[5]

According to Rau, azobenzenes can be divided into three main categories: "azobenzenes," "amino-azobenzenes," and "pseudostilbenes."[6] This classification is based on the relative energies of the n–π^* and π–π^* transitions.[7,8] Azobenzene molecules show an intense π–π^* band in the UV region at 350 nm followed by a weak n–π^* band at 440 nm. In the case of the amino-azobenzenes, the π–π^* band is red-shifted to the proximity of the n–π^* band, which is insensitive to substituent effects, thereby causing a partial overlap of both bands.[9] Unlike the preceding categories, pseudostilbenes are substituted with strong electron-donor and electron-withdrawing groups. Therefore, they are also named push–pull molecules; the π–π^* and the n–π^* are inverted in the energy scale and totally overlap so that only one absorption band is observed. Moreover, for this kind of azobenzenes, the

photoisomerization is reversible, very fast, and takes place in the order of picoseconds. Thus, pseudostilbenes can reversibly isomerize trans–cis as long as they are illuminated with linear polarized light in the UV–vis range.

In the last years, various azopolymers bearing amino-nitro-substituted azobenzene units, flexible alkyl spacers, and a polymethacrylate backbone such as those of the pnMAN series, have been synthesized and characterized.[10] In general, they exhibit absorption maxima at wavelengths close to those reported for similar push–pull azocompounds.[11,12] These kinds of materials easily form J- and H-type aggregates in cast films.[10] Nevertheless, acrylic azomonomers usually exhibit slightly lower reactivity toward polymerization than other analogous monomers without azobenzene. It has been already reported in the literature that the homopolymerization of azomonomers usually give polymers with medium to low molecular weights.[10]

Previously, we reported the synthesis, characterization, and optical properties of a series of novel amphiphilic amino-nitro-substituted azo-dyes and azopolymers bearing oligo(ethylene glycol) segments.[13–16] Azobenzene and poly(ethylene glycol) have been incorporated into various sophisticated systems such as copolymers,[17,18] nanomaterials,[19,20] cellulose derivatives,[21,22] and cyclodextrin polymers,[23,24] sometimes forming supramolecular complexes with interesting properties.[25]

Frontal polymerization (FP) is a process in which polymerization occurs directionally.[26] There are mainly three types of FP: the first is the isothermal one; the second is the photofrontal polymerization, in which the front is driven by the continuous flux of radiation, usually UV-light; the last one is the thermal FP, which results from the application of heat in a specific point of the reactor. One of the most important conditions to successfully carry out an FP is that the system must be inert at room temperature but very reactive once ignited, thus quickly releasing a sufficient amount of heat to generate a self-sustaining propagating reaction front that converts monomer into polymer.

FP was discovered in Russia by Chechilo and Enikolopyan in the 1970s,[27] and their work was pushed further in 1984.[28] Our group has used this technique for the consolidation of porous materials,[29,30] to synthesize interpenetrating polymer networks,[31] unsaturated polyester/styrene resins,[32,33] hydrogels,[34–37] polymer-based nanocomposites,[38] and polyhedral oligomeric silsesquioxanes.[39] In our most recent articles, we used FP to synthesize hybrid inorganic/organic epoxy resins,[40] to obtain stimuli-responsive hydrogels containing partially exfoliated graphite,[41] and to copolymerize successfully an azomonomer into two different polymer matrices.[42,43] Recently, we reported that FP could be used to obtain materials that cannot be prepared by the classical method; namely, graphene-containing nanocomposite hydrogels of poly(*N*-isopropylacrylamide) were synthesized. In particular, at variance to what was found using the classical polymerization technique, by FP graphene did not reaggregate to graphite flakes, thereby allowing the preparation of a homogeneously dispersed nanocomposite.[44]

Chen et al. proposed FP as the technique for the polymerization of 2-hydroxyethyl acrylate,[45] epoxy resin/polyurethane networks,[46] vinylpyrrolidone,[47] quantum dot polymer nanocomposites,[48] and polyurethane-nanosilica hybrid nanocomposites.[49] Lastly, they have also obtained amphiphilic gels,[50] and hydrogels of *N*-vinylimidazole for adsorption of metals.[51]

In addition, Pojman et al. published a review covering the most important features in FP up to 1996.[52] Moreover, they investigated the instability of the front,[53,54] the influence of the spin modes and the reactor geometry in FP,[55] the FP of poly(dicyclopentadiene),[56] urethane acrylates,[57] acrylic monomers,[58–60] the use of a microencapsulated initiator,[61] and the formation of simultaneous-interpenetrating polymer networks.[62] Lately, they developed the frontal cationic curing of an epoxy resin[63] and studied the FP of a triacrylate with inert phase-change materials.[64]

In this article, we report the FP of bisphenol A ethoxylate diacrylate (BPAEDA), using the ionic liquid trihexyltetradecylphosphonium persulfate (TETDPPS) as radical initiator, which was previously synthesized by us.[65] Additionally, we have incorporated two azobenzene-containing comonomers, namely, (E)-2-(ethyl(4-((4-nitrophenyl) diazenyl) phenyl) amino)ethyl methacrylate (MDR-1) and (E)-2-(4-((4-nitrophenyl)diazenyl)phenyl)-5,8,11-trioxa-2-azatridecan-13-yl methacrylate (4PEGMAN; see structures in Scheme 1). The obtained copolymers were characterized by FTIR spectroscopy, and their thermal properties were determined by thermogravimetric analysis (TGA) and differential scanning calorimetry (DSC). Moreover, the optical properties of the two series of copolymers were studied by absorption spectroscopy in the UV–vis range. Finally, the cubic NLO-characterizations of the obtained BPAEDA/MDR-1 and BPAEDA/4PEGMAN amorphous copolymers were performed according to the Z-Scan technique in thin-film samples prepared by classical polymerization.[66]

RESULTS AND DISCUSSION

The FP of BPAEDA was carried out using different initiators: benzoyl peroxide (BPO), 2,2′-azobis isobutyronitrile (AIBN), aliquat persulfate® (APS), and the ionic liquids tetrabutylphosphonium persulfate (TBPPS) and TETDPPS.

First, we tested different kinds of initiators for the FP of BPAEDA. As BPO and TBPPS were not able to self-sustain a propagating front with the same concentration with which TETDPPS did, the minimum quantities of such initiators were not determined because they proved to be useless in this work. In the case of APS and AIBN, it was necessary to use 0.57 and 3 mol % of them, respectively, to succeed in performing an FP. In addition, samples obtained with AIBN were full of bubbles and inadequate for our study on optical properties; and those with APS were not useful because a very high concentration of initiator is required to promote a polymerization front, contrary to what happens with the TETDPPS initiator. Finally, the ionic liquid TETDPPS was found to promote FP with an almost constant velocity, with respect to its concentration, and relatively low temperatures

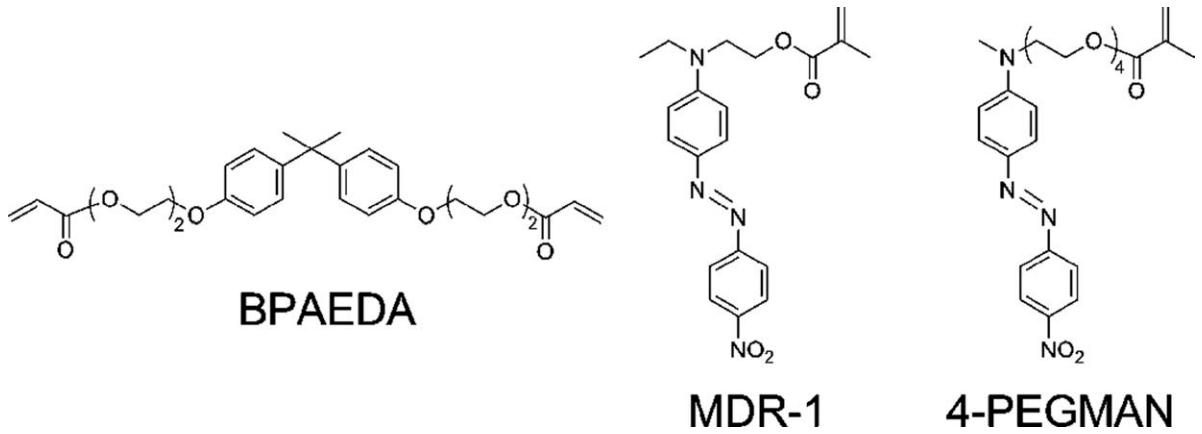

SCHEME 1 Structure of the used monomers, BPAEDA, MDR-1, and 4PEGMAN.

of the propagating front, thus avoiding bubble formation and any possible thermal degradation. This initiator was used in lower quantity (0.44% mol) than those used with other initiators used in this work. Therefore, herein, we report the results obtained with this initiator.

From the set of results presented in Table 1, it was determined that an increase of TETDPPS concentration increased both the front velocity (V_f) and the maximum temperature (T_{max}) reached by the propagating front. Moreover, conversion from monomer into polymer was found to be between 84 and 94%, without any apparent relationship with the TETDPPS concentration.

Meanwhile, Table 2 shows the results of the frontal copolymerization of BPAEDA with the azomonomer MDR-1, using TETDPPS as initiator. The front velocity exhibits values between 0.9 and 1.3 cm min^{-1}, which are higher than that found in BPAEDA homopolymerization (0.7 cm min^{-1}). Analogously, when MDR-1 was added T_{max} and conversion also increase (from 134 up to 145 °C, and from 84 up to 97%, respectively).

Table 3 shows the results of the frontal copolymerization of BPAEDA and 4PEGMAN using TETDPPS as initiator. As we can see, all the front velocity data of the copolymers showed values between 0.85 and 1.0 cm min^{-1}, which are slightly faster than that of the BPAEDA homopolymer ($V_f = 0.7$ cm min^{-1}).

TABLE 1 Front Velocity Values, Maximum Reached Temperatures, Glass Transition Temperatures, and Conversion Values of the Obtained Polymers in the Frontal Polymerization of BPAEDA, Varying the TETDPPS Concentration

TETDPPS (mol %)	V_f (cm min^{-1})	T_{max} (°C)	T_g (°C)	Conversion (%)
0.33	0.6	128	51	92
0.44	0.7	134	51	84
0.65	1.0	140	45	85
0.87	1.1	142	42	89
1.10	1.3	147	44	94

Moreover, the maximum temperature reached by the front also slightly increased from 134 to 141 °C as consequence of PEGMAN addition. As well as in the case of the polymerization of BPAEDA, the conversion remained between 84 and 93%. However, the glass transition temperature of the obtained polymers decreased from 51 to 34 °C, when 4PEGMAN monomer was incorporated into the poly-BPAEDA matrix.

The optical properties of the copolymers were studied by UV–vis spectroscopy, and the absorption spectra of the copolymers prepared with the two aforementioned azomonomers are shown in Figures 1 and 2. In the case of the copolymers bearing MDR-1 units in their structure, all of them exhibited a maximum absorption band around $\lambda_{max} =$ 463–468 nm (not shown), which is 10-nm blue-shifted with respect to the MDR-1 absorption in $CHCl_3$ ($\lambda_{max} =$ 472–474 nm). This slight hypsochromic effect reveals the presence of traces of H-aggregates between the azobenzene groups in the polymer. These results confirmed the incorporation of MDR-1 into the poly-BPAEDA structure (Fig. 1).

Meanwhile, the azomonomer 4PEGMAN exhibits a maximum absorption band in $CHCl_3$ solution at $\lambda_{max} = 480$ nm. In the case of the copolymers of BPAEDA/4PEGMAN, all of them

TABLE 2 Front Velocity Values, Maximum Reached Temperatures, Glass Transition Temperatures, and Conversion Values for the Copolymers in the FP of BPAEDA and MDR-1 Azomonomer, Using TETDPPS (0.44 mol %) as Initiator

MDR-1 (mol %)	V_f (cm min^{-1})	T_{max} (°C)	T_g (°C)	Conversion (%)
0	0.7	134	51	84
0.014	1.2	145	53	92
0.034	1.3	148	49	88
0.077	1.1	145	47	97
0.10	1.1	145	51	93
0.13	0.9	142	49	93
0.33	0.9	141	47	91

TABLE 3 Front Velocity Values, Maximum Reached Temperatures, Glass Transition Temperatures, and Conversion Values of the Obtained Polymers in the Frontal Copolymerization of BPAEDA and 4PEGMAN, Using TETDPPS (0.44 mol %) as Initiator

4PEGMAN (mol %)	V_f (cm min^{-1})	T_{max} (°C)	T_g (°C)	Conversion (%)
0	0.7	134	51	84
0.010	0.95	139	52	89
0.026	0.85	136	49	93
0.050	0.96	139	46	93
0.080	0.97	140	34	89
0.10	1.00	141	39	85
0.26	0.88	138	43	85

(not shown) exhibited a maximum absorption band in the same solvent at λ_{max} = 472–474 nm, which is 8-nm blue-shifted with respect to that of the azomonomer. Similarly, this hypsochromic effect confirms also the presence of H-aggregates between the azobenzene groups in these polymers (Fig. 2).

As MDR-1 and 4PEGMAN, like other amino-nitro-substituted azobenzenes, belong to the pseudostilbenes category of the Rau's classification, they exhibit a total overlap of the π–π^* and n–π^* bands so that only a blue-shift of the maximum absorption band can be observed.

Since, from a comparison between the samples obtained by FP and by classical bulk polymerization, it was found that their optical properties are absolutely similar, FP was used to obtain thick samples, which might have practical applications in optical storage, photolithography, and the elaboration of other optical devices. However, given that the study of NLO properties by means of the Z-scan technique requires the use of thin films, these were prepared by classical bulk polymerization.

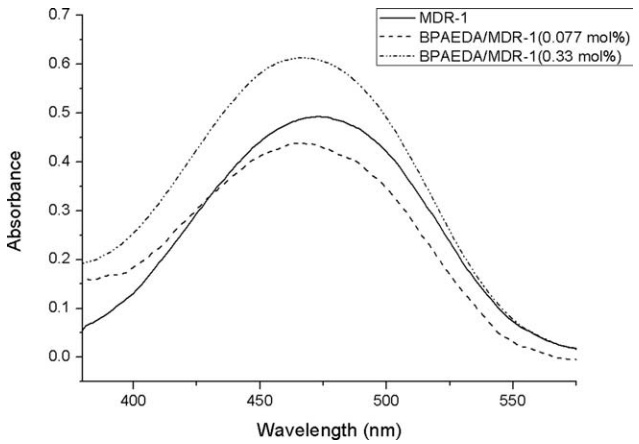

FIGURE 1 UV–vis spectra of the azomonomer MDR-1 and of two 2-PEA/MDR-1 copolymers with different azomonomer concentrations [MDR-1 = 0.077 and 0.33 mol %] [TETDPPS = 0.44 mol %].

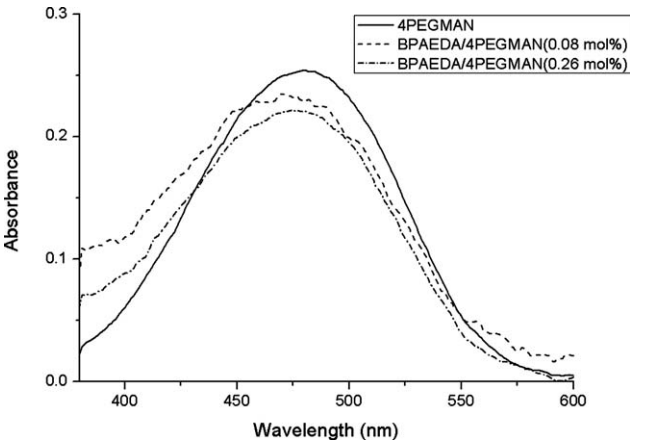

FIGURE 2 UV–vis spectra of the azomonomer 4PEGMAN and of two 2-PEA/4PEGMAN copolymers with different azomonomer concentrations [4PEGMAN = 0.08 and 0.26 mol %] [TETDPPS = 0.44 mol %].

Namely, the linear absorption coefficients evaluated within the visible range for the BPAEDA/MDR-1 and BPAEDA/4PEGMAN copolymer films with higher MDR-1 and 4PEGMAN chromophore content (at 0.33 and 0.26 mol %, respectively) are shown in Figure 3(a,b). The thickness of the studied samples (sandwiched films prepared within two glass slices) was in the order of ~60–80 μm; thus, the Lambert–Beer law applies for such semitransparent film structures, allowing an adequate data analysis and making these copolymers potential candidates for some optical applications due to their appropriate transparency at optical wavelengths. It is evident from Figure 3(a,b) that the highest absorptive properties of the copolymer samples occur within the 400–580 nm spectral range in both BPAEDA/MDR-1 and BPAEDA/4PEGMAN films. In contrast, the pristine BPAEDA reference film (RF) does not exhibit significant absorption within the whole spectral range. This fact indicates the successful copolymerization of the MDR-1 and 4PEGMAN with the BPAEDA matrix using TETDPPS as ionic liquid initiator. Indeed, the absorption properties of these copolymers points to additional conjugation of delocalized π-electrons provided by the higher content of push–pull chromophores in these systems, this assumption will be explored by means of cubic NLO Z-Scan experiments as explained below. Under this framework, the available laser excitation line implemented in Z-Scan experiments ($\lambda_{Z\text{-}Scan}$ = 632.8 nm) is also shown in Figure 3(a,b) (vertical dashed lines). At this wavelength, the copolymer samples exhibit lower absorption conditions, allowing nonresonant cubic NLO-characterizations of the developed films, which represent a critical point when working with organic materials, showing moderate to low T_g values. Indeed, relatively small linear absorption coefficients in the order of $\alpha_0 \approx$ 800–1500 m^{-1} (see values in Table 4) were evaluated for the studied copolymer films at $\lambda_{Z\text{-}Scan}$. These values are very useful for the determination of the nonlinear refraction and absorption coefficients according to the Z-Scan experimental technique

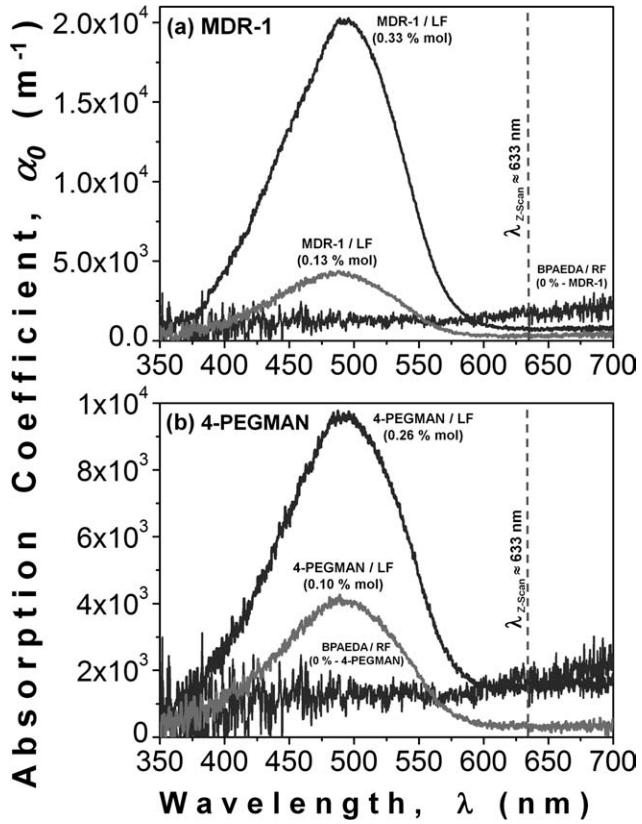

FIGURE 3 (a and b) Comparative linear absorption coefficients obtained for the pristine BPAEDA reference film (RF) and the BPAEDA/MDR-1 and BPAEDA/4PEGMAN copolymer films samples (labeled films: LF) prepared with the TETDPPS ionic liquid initiator at different MDR-1 and 4PEGMAN chromophore concentrations: (a) BPAEDA/MDR-1 copolymer film samples prepared at 0.33 and 0.13 mol % (MDR-1) and (b) BPAEDA/4PEGMAN copolymer film samples prepared at 0.26 and 0.10 mol % (4PEGMAN).

The Z-Scan NLO-measurements were performed at room conditions on the developed BPAEDA/MDR-1 and BPAEDA/4PEGMAN copolymer thin films. Measurements include the Z-Scan signals obtained from the reference poly-BPAEDA film (RF) and the cover slip glass substrates to monitor the NLO-activity of the polymer matrix and the influence of photoactive units on the copolymer film systems. The observed nonlocal effect of these samples is shown in Figure 4(a,f). A rigorous theoretical fitting was performed to simultaneously evaluate both the nonlinear absorptive and refractive properties of these samples. The NLO-response of the studied films was characterized by varying the input polarization planes of the laser beam to explore microscopic material asymmetries or anisotropies throughout the film structure; measurements were also performed on several regions of the specimens to rigorously verify the experimental results. In general, as all NLO-measurements were systematically performed with different input polarization states (from 0 to 90°: *S*- and *P*-polarization, respectively) and the obtained curves are quite similar in each sample, the film structures do not seem to

TABLE 4 Structural, Linear and Cubic NLO-Parameters Obtained for the BPAEDA/MDR-1 and BPAEDA/4PEGMAN Copolymer Films (With the Highest Chromophore Content, i.e., MDR-1 = 0.33 mol % and 4PEGMAN = 0.26 mol %) According to UV–vis Optical Spectroscopy and the NLO/Z-Scan Technique (Closed Aperture Z-scan Measurements at $\lambda_{Z\text{-Scan}} \approx 633$ nm, $S \approx\approx 19\%$, Rayleigh range $z_0 \approx 3.1$ mm, Laser power: ~6.3 mW)

Film Sample	BPAEDA Chromophore Concentration (mol %)	Film Thickness (μm)	Linear Absorption Coefficient: α_0 at $\lambda = 632.8$ nm (m^{-1})	$\Delta\Phi_0/\Delta\Psi_0$	NLO Refractive Index: γ/n_2 at $\lambda = 632.8$ nm × 10^{-10} (m^2 W^{-1}) [$\times 10^{-4}$ (esu)]	NLO Absorption Coefficient: β (TPA or SA) ($\times 10^{-4}$ m W^{-1})
BPAEDA/RF	100:0	18.13	1,577.7	−0.37/0.0	−1.80/−6.70	0.0
BPAEDA/MDR-1–LF	100:0.33	76.25	792.5	−0.19/0.0	−0.20/−0.71	0.0
BPAEDA/4PEGMAN–LF	100:0.26	58.75	1,681.9	+0.54/−0.02	+0.83/+3.14	−0.62 (SA)

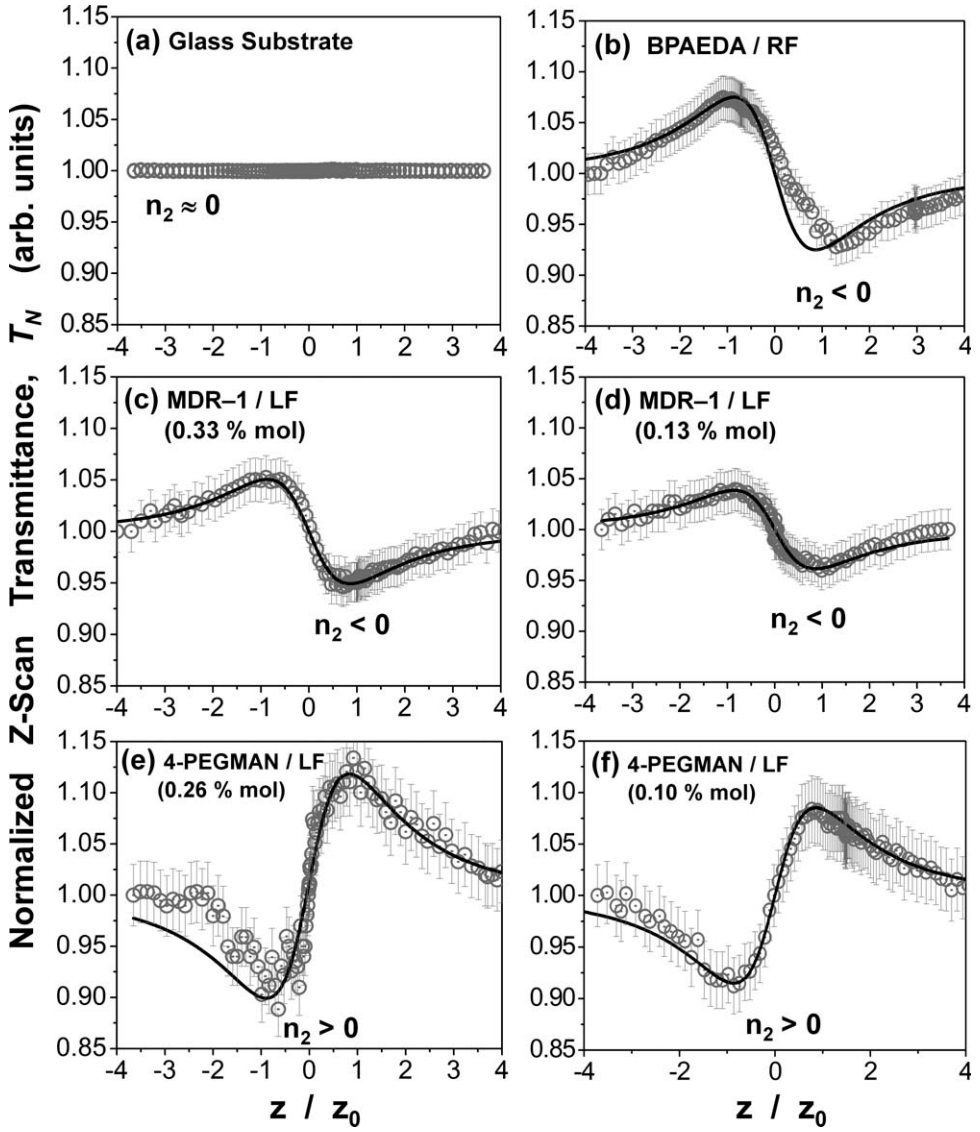

FIGURE 4 (a–f) Closed aperture Z-Scan data (scattered points) and theoretical fitting (continuous lines) obtained at $\lambda_{Z\text{-Scan}} = 632.8$ nm for: (a) the glass substrates, (b) the pristine BPAEDA reference film (RF), (c and d) the BPAEDA/MDR-1 based copolymer films (labeled films: LF) prepared with different MDR-1 chromophore content (at 0.33 and 0.13 mol %, respectively), and (e and f) the BPAEDA/4PEGMAN based copolymer films (labeled films: LF) prepared with different 4PEGMAN chromophore content (at 0.26 and 0.10 mol %, respectively). An estimated experimental error below 3% is also considered for the Z-Scan data (error bars).

show any significant anisotropic behavior, thereby confirming their amorphous nature. On the other hand, as the studied samples have a moderate glass transition temperature (T_g values around 45 °C), the Z-Scan curves and related NLO-effects were obtained at relatively low laser intensities.

Taking into account the theory developed by Sheik-Bahae et al. and Liu et al.,[67–71] it is observed from our measurements that the nonlinear refractive response of the studied samples can be unambiguously determined by typical peak-to-valley Z-Scan transmittance curves. Hence, one can immediately observe that the cover slip glass substrate exhibits a negligible nonlinear refractive effect (flat Z-Scan curve: NLO-refractive coefficient $n_2 \approx 0$, see Figure 4(a). On the other hand, the highly transparent poly-BPAEDA RF (polymer matrix) clearly exhibits a negative NLO-refractive activity (peak-to-valley Z-Scan transmittance curve: $n_2 < 0$, see Figure 4(b). Finally, the BPAEDA/MDR-1 and BPAEDA/4PEGMAN copolymer film samples (labeled films: LF) also exhibit well-defined Z-Scan experimental curves, which anticipate interesting NLO-refractive properties with a reversal of the NLO-behavior detected for the BPAEDA/4PEGMAN copolymer films. As the cover slip glass substrates implemented to sandwich the copolymer films do not contribute to the NLO-effects at the implemented laser power regime ($\sim 1.16 \times 10^7$ W m^{-2}), it is assumed that the change of the NLO-refractive response of the labeled samples is mainly promoted by the poly-BPAEDA and by a successful copolymerization of the NLO-active MDR-1 and 4PEGMAN monomers with the

BPAEDA main monomer using TETDPPS. Particularly, in the case of the BPAEDA/MDR-1 copolymer films [see Fig. 4(c,d)], samples prepared with different MDR-1 concentrations (0.33 and 0.13 mol %, respectively) consistently exhibit the same NLO-tendency as the pristine BPAEDA-film sample (with $n_2 < 0$). Indeed, the BPAEDA/MDR-1 copolymer films also show negative NLO-refractive properties, which indicate a strong dependence on the NLO-behavior of the poly-BPAEDA matrix. In contrast, the BPAEDA/4PEGMAN copolymer films prepared with different 4PEGMAN chromophore concentrations (0.26 and 0.10 mol %, respectively) exhibit different NLO-properties [see Fig. 4(e,f)]. In this case, the NLO-experimental data consistently show inverted valley-to-peak Z-Scan transmittance curves pointing to strong and positive NLO-refractive properties ($n_2 > 0$). This sign reversal of the NLO-refractive index also indicates that the NLO-activity of the BPAEDA/4PEGMAN copolymer films mainly depend on the intrinsic NLO-properties of the 4PEGMAN units and not on the BPAEDA units of the polymer matrix. In other words, the positive NLO-activity of the 4PEGMAN units is high enough to reverse the NLO-effect of the poly-BPAEDA matrix. As a matter of fact, according to the structural results obtained from molecular modeling, the 4PEGMAN monomer has a stronger dipole moment ($\mu_{4PEGMAN} \approx 9.4$ D) than that obtained for MDR-1 ($\mu_{MDR\text{-}1} \approx 6.8$ D). Thus, a higher NLO-response is expected for the BPAEDA/4PEGMAN copolymer films because the NLO-behavior of organic compounds is, in general, governed by their inherent charge-transfer properties.

The respective theoretical fits (TFs) of the obtained Z-Scan transmission data (solid lines) are also shown in Figure 4(a–f). According to previous theoretical studies, the normalized Z-Scan transmittance (T_N) can be determined as a function of the dimensionless sample position ($x = z/z_0$), where z_0 is the Rayleigh range and z is the Z-Scan sample position (laboratory reference frame). Hence, the TFs were performed according to the following equation (considering both nonlinear refraction and absorption effects):[67]

$$T_N \approx 1 + [4x/(1+x^2)(9+x^2)]\Delta\Phi - [2(x^2+3)/(1+x^2)(9+x^2)]\Delta\Psi \quad (1)$$

Here, the first term represents a normalization factor, the second term is related to NLO-refractive effects whereas the third one is associated to NLO-absorptive phenomena. Hence, the fitting parameters are the induced phase shifts $\Delta\Phi$ or $\Delta\Psi$, respectively. In the former case, the phase shift is given by $\Delta\Phi = 2\pi\gamma I_0 L_{eff}/\lambda$,[67] from which the NLO-refractive index (n_2- or γ-coefficient) can be obtained. In the latter case, the phase shift is provoked by the NLO-absorptive phenomena and is given by $\Delta\Psi = \beta I_0 L_{eff}/2$,[67] allowing the evaluation of the NLO absorption (β-coefficient) either due to two photon (or multiphoton) NLO-absorption or to saturated NLO-absorption. In these equations, λ is the laser wavelength, I_0 is the input beam intensity (at focal spot: $z = 0$) and L_{eff} is the effective thickness of the film sample defined as $L_{eff} = [1 - (e^{-\alpha_0 L_S})](\alpha_0)^{-1}$ (where α_0 represents the linear absorption coefficient). All these equations are well established and have been proven in early Z-Scan works.[67–72] The theoretical restrictions imposed by these formulas to apply such expressions at optimal conditions ($|\Delta\Phi_0| < \pi$, $S \approx 20\%$, etc.) are not always fully satisfied in our experimental results due to the large phase shifts and huge nonlinearities obtained in our experiments. Nevertheless, in most cases (mainly in the case of well-defined $\gamma > 0$ or $\gamma < 0$ curves), our experimental data nearly satisfy these conditions and can be conveniently fit according to these theoretical expressions. Thus, for comparison purposes and to be consistent with the estimation of the γ- and β-values, we assumed their applicability and used them to fit our experimental results. The TFs allowed us to evaluate a large negative NLO-refractive coefficient in the order of $\gamma = -1.80 \times 10^{-10}$ m^2 W^{-1} (or $n_2 = -6.70 \times 10^{-4}$ esu) for the poly-BPAEDA-RF and $\gamma = +0.83 \times 10^{-10}$ m^2 W^{-1} (or $n_2 = +3.14 \times 10^{-4}$ esu) for the BPAEDA/4PEGMAN copolymer film (at higher 4PEGMAN content: 0.26 mol %, see results in Table 4). The obtained γ/n_2-values are very large, many orders of magnitude larger than those observed for typical glass substrates or for the classical CS_2 standard NLO-reference material: $+1.2 \times 10^{-11}$ esu (Z-Scan at $\lambda = 10.6$ μm) or 6.8×10^{-13} esu (degenerate four-wave mixing at $\lambda = 532$ nm).[68–72]

On the other hand, as the Z-Scan experimental data exhibit well-defined and symmetric peak-to-valley or valley-to-peak transmittance curves, NLO absorption effects are not expected.[67] Indeed, according to the TFs, only a small NLO-absorption coefficient of $\beta \approx -0.62 \times 10^{-4}$ m W^{-1} was estimated for the BPAEDA/4PEGMAN copolymer film prepared with the highest chromophore content (0.26 mol %). The sign of the β-coefficient reveals the nature of the NLO-absorptive phenomenon occurring in this sample. In fact, the negative sign indicates that moderate saturated absorption (SA) effects take place within the BPAEDA/4PEGMAN copolymer film samples.[68–72] This result indicates convenient material properties to avoid undesired photothermal effects such as photodegradation and molecular reorientation during Z-Scan experiments due to long cw-laser irradiation and low T_g values of the samples.

EXPERIMENTAL

Materials

BPAEDA ($M_n \approx 512$, $d = 1.14$ g mL^{-1}), tetraethylene glycol (FW = 194.23, $d = 1.125$ g mL^{-1}), *p*-toluenesulfonyl chloride (FW = 190.65, mp = 66 °C, bp = 134 °C), 4-nitrobenzenediazonium tetrafluoroborate (FW = 236.92, mp = 150 °C), triethylamine (TEA, FW = 101.19, bp = 88.8 °C, $d = 0.726$ g mL^{-1}) and disperse red-1 dye (DR-1, FW = 314.34, mp = 160–162 °C) were purchased from Sigma-Aldrich. *N*-Methylaniline (FW = 107.15, $d = 0.989$ g mL^{-1}), tetrabutylphosphonium chloride (FW = 294.89, mp = 62–66 °C), trihexyltetradecylphosphonium chloride (FW = 519.31, $d = 0.895$ g mL^{-1}), BPO (FW = 242.23, mp = 102–105 °C), and methacryloyl chloride (MAC, FW = 104.53, bp = 95–96 °C, $d = 1.07$ g mL^{-1}) were purchased from Fluka. All reagents used in the polymer synthesis were used as received,

without further purification. The azomonomer (MDR-1),[73,74] *N*-methyl-*N*-{4-[(E)-(4-nitrophenyl)diazenyl]phenyl}-*N*-(11-hydroxy-3,6,9-trioxaundecas-1-yl) amine (RED-PEG-4) dye,[13] aliquat persulfate® (APS),[75] and the ionic liquids TBPPS and TETDPPS[65] were synthesized according to the procedures previously described in the literature.

Synthesis of (E)-2-(4-((4-Nitrophenyl)diazenyl)phenyl)-5,8,11-trioxa-2-azatridecan-13-yl Methacrylate

RED-PEG-4 dye (2.28 mmol) was dissolved in freshly distilled THF (12 mL) under argon atmosphere; then TEA (0.33 g, 3.32 mmol) was added with a syringe to the solution. The mixture was cooled in an ice bath, and MAC (0.29 g, 2.76 mmol) dissolved in THF (4 mL) was added dropwise by the means of an addition funnel. The reaction mixture was stirred for 24 h at room temperature. The resulting product was extracted with chloroform, dried with anhydrous $MgSO_4$, and concentrated at reduced pressure. Then, the crude product was purified by flash column chromatography on silica gel, using an appropriate mixture hexane–acetone as eluent. Pure 4PEGMAN monomer was obtained as a dark red solid. Yield: 82%. The structure of 4PEGMAN was confirmed by FTIR, ^{1}H NMR, and ^{13}C NMR spectroscopies.

IR (KBr): ν = 3090 (s, C—H aromatic and vinylic), 2961 (s, CH_2), 2924 (s, CH_2 and CH_3), 1727 (s, C=O), 1603 (s, C=C aromatic), 1516 (s, NO_2), 1447 (s, N=N), 1378, 1337 (s, C—O of the esther), 1261(s, C—N), 1099 (s, O—CH_2), 856 (out of plane, =CH_2 vinylic), 802 (out of plane, =C—H aromatic) cm^{-1}.

^{1}H NMR ($CDCl_3$, 400 MHz) (Scheme 2): δ = 8.31 (d, 2H, J = 9.3 Hz, H^4); 7.98 (dd, 4H, J = 8.7 Hz, H^3 and H^2); 6.83 (d, 2H, J = 9.3 Hz, H^1); 6.12 (s, 1H, H^5); 5.57 (s, 1H, H^6); 4.30 (t, 2H, J_1 = 4.8 Hz, J_2 = 4.8 Hz, COO—CH_2); 3.72, 3.63 (m, 14H, all OCH_2 and NCH_2); 3.19 (s, 3H, CH_3—N); 1.94 (s, 3H, =C—CH_3) ppm.

^{13}C NMR ($CDCl_3$, 100 MHz) (Scheme 2): δ = 186.2 (1C, C=O), 156.82 (1C, C^e), 153.35 (1C, C^a), 147.17 (1C, C^h), 143.01 (1C, C^d), 136.10 (1C, C= of the methacrylate), 127.36 (1C, CH_2= of the methacrylate), 125.71 (2C, C^c), 124.7 (2C, C^g), 122.17 (2C, C^f), 112.17 (2C, C^b), 72.39, 70.82, 70.59, 70.56, 70.22, 68.49 (6C, OCH_2), 63.77 (1C, CH_2OCO), 52.53 (1C, N—CH_2), 39.67 (1C, CH_3—N), 18.28 (CH_3 of the methacrylate) ppm.

Frontal Polymerization Experiments

FP experiments were performed as follows: in a glass test tube (16 cm length, 16 mm diameter), a suitable amount of monomer (BPAEDA) with or without azo-comonomer (MDR-1 or 4PEGMAN), and initiator (TETDPPS) were placed without any solvent and mixed until all the initiator was completely dissolved.

The tubes containing the reaction mixture were locally heated at the top level of the solution, using a soldering iron as the external heating source, until the formation of a propagating front was evident. The heat released during the conversion of the monomer into polymer was responsible for the formation of a hot front, able to self-sustain the polymerization process and the propagation throughout the whole tube. Front velocity (±0.05 cm min^{-1}) and front maximum temperature (±10 °C) were recorded.

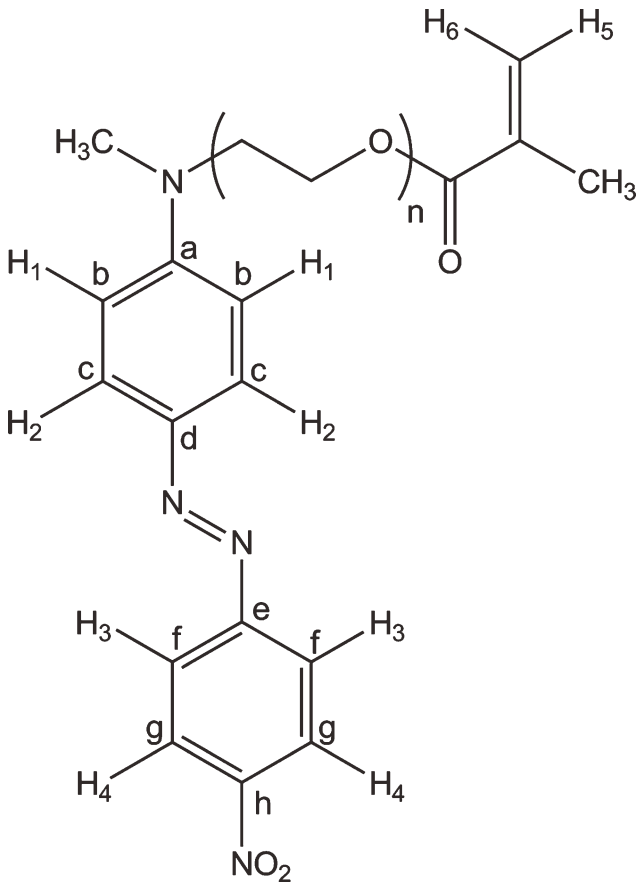

SCHEME 2 Structure of the MDR-1 with the assigned H for NMR characterization.

Temperature profiles were measured using a K-type thermocouple placed in the monomer-initiator mixture above 2 cm (±0.5 cm) from the bottom of the tube. This thermocouple was connected to a digital thermometer (Delta Ohm 9416), which was used for temperature reading. The position of the front, easily visible through the glass walls of the tube, was measured as a function of time.

Characterization

Once the polymerizations were achieved, the obtained samples were removed from the tubes and analyzed by DSC to determine the conversion percentage, which was always found to be almost quantitative.

DSC measurements were conducted in a DSC Q100 Waters TA Instrument. For each sample, two consecutive scans were carried out from −80 to +300 °C, under argon atmosphere, with a heating rate of 10 °C min^{-1}. Monomer conversion was determined by the following equation:

$$\text{Conversion}\ (\%) = [1 - (\Delta H_r/\Delta H_t)] \cdot 100$$

where ΔH_r (residual) is the peak area obtained for the residual polymerization after the first thermal scan, and ΔH_t

(total) is the area under the curve when the polymerization was carried out in the DSC instrument, and corresponding to the complete conversion.

TGA measurements were performed using a TA instrument thermobalance TGA 2050, under inert atmosphere, from 25 to 500 °C with a heating rate of 10 °C min^{-1}. Absorption spectra of the azomonomers ($CHCl_3$ solution, 1-cm quartz cell) and the copolymers (solid state) were recorded in a Hitachi U-2010 spectrometer. This technique was useful to determine the MDR-1 or 4PEGMAN content in all polymer samples. The extinction coefficient of the azomonomers MDR-1 and 4PEGMAN in $CHCl_3$ solution were estimated to be 46,700 M cm^{-1}.

The FTIR spectra of the monomer and the corresponding polymer (not shown) were recorded with a Fourier transform infrared spectrometer (JASCOFT 480) in KBr pressed pellets. For each sample, 16 scans were recorded at a resolution of 4 cm^{-1}. ^1H and ^{13}C NMR spectra of the monomers in $CDCl_3$ solution were recorded at room temperature on a Bruker Avance 400 MHz spectrometer, operating at 400 and 100 MHz for ^1H and ^{13}C, respectively.

Finally, the obtained BPAEDA/MDR-1 and BPAEDA/4PEGMAN copolymers were also studied in thin-film samples prepared by classical polymerization (100 °C, ca. 72 h) using the same mixture compositions as that used for the obtainment of the other samples. Their cubic $\chi^{(3)}$-NLO effects such as nonlinear refraction and nonlinear absorption were studied using the Z-Scan technique.[66] The experimental Z-Scan setup was implemented using a cw-unpolarized laser beam from a 35-mW He-Ne laser system working at 632.8 nm (THORLABS, HRR170-1). Its energy was carefully monitored and kept constant during long Z-Scan measurements. The spatial mode of the laser beam was close to Gaussian TEM_{00}. The polarization plane of the laser beam was adjusted and controlled by means of a linear polarizer mounted on a rotation stage. The polarized laser beam was focused on the sample by means of a positive lens ($f = 5$ cm), so that a light power density of $\sim 1.16 \times 10^7$ W m^{-2} reached the studied samples at the focal spot. The film samples were mounted on a motorized translation stage (25-mm length travel in steps of 2 μm) to perform Z-Scan experiments within the focal range. A large area Si-photodetector (EOT ET-2040) was located at ~0.96 m from the focusing lens, after a 2.5-mm diameter (~20% transmittance) diaphragm-aperture. All NLO-signals captured from photodetectors were recorded with a digital oscilloscope (Tektronix TDS, 744A); the whole Z-Scan setup was automated via a LabView control program for data acquisition.

CONCLUSIONS

In this work, BPAEDA was frontally copolymerized with (E)-2-(ethyl(4-((4-nitrophenyl)diazenyl)phenyl)amino)ethyl methacrylate or 4PEGMAN. The use of TETDPPS as radical initiator allowed us to obtain polymer samples that were completely free of bubbles. Moreover, to study their cubic NLO-refractive properties, we also prepared thin films by classical polymerization using this initiator. They were measured via the Z-Scan technique in the BPAEDA/4PEGMAN and BPAEDA/MDR-1 copolymer film samples. Indeed, although the reference poly-BPAEDA exhibits an intrinsic and non-negligible negative NLO-refractive activity, the BPAEDA/4PEGMAN copolymer samples were able to reverse the sign of the nonlinearity to show strong and positive NLO-refractive coefficients in the order of $+3 \times 10^{-4}$ esu. All film samples exhibited remarkably stable NLO-activity under cw-laser excitation, and the respective theoretical fittings were satisfactorily correlated to the experimental data. This was mainly due to the relatively good thermal properties of the copolymers and the poly-BPAEDA network, and to the optimal azomonomer incorporation via FP, using TETDPPS as catalyst. However, more NLO-studies should be performed in these materials to deeply understand the electronic contributions of the implemented push–pull chromophores to the cubic nonlinearities. Additionally, complementary studies on the chromophore addition to the BPAEDA polymer matrix should be also performed to improve both the NLO-response and thermal properties for enhanced photonic applications (including quadratic NLO-applications such as second harmonic generation (SHG) in electrically poled film samples).

The authors thank Gerardo Cedillo and Miguel Angel Canseco for their assistance with NMR and absorption spectroscopies, respectively. The authors also thank Esteban Fregoso Israel for their assistance with DSC and TGA measurements. Javier Illescas, Jesus Ortíz-Palacios, Jair Esquivel-Guzmán, and Yessica S. Ramírez-Fuentes are grateful to CONACyT for scholarship. The authors also thank PAPIIT-DGAPA (Project IN-105610), the Instituto de Ciencia y Tecnología del Distrito Federal (ICyTDF), and the Italian Ministry of University and Scientific Research for financial support.

REFERENCES AND NOTES

1 Natansohn, A.; Rochon, P. *Chem. Rev.* **2002,** *102*, 4139–4175.

2 Ichimura, K. *Chem. Rev.* **2000,** *100*, 1847–1873.

3 Delaire, J. A.; Nakatani, K. *Chem. Rev.* **2000,** *100*, 1817–1845.

4 Sourisseau, C. *Chem. Rev.* **2004,** *104*, 3851–3891.

5 Kumar, G. S.; Neckers, D. C. *Chem. Rev.* **1989,** *89*, 1915–1925.

6 Rau, H. In Photoreactive Organic Thin Films; Sekkat, Z.; Knoll, W., Eds.; Zouheir Sekkat; Wolfgang Knoll, Academic Press-Elsevier Science, USA, **2002, 3–48.**

7 Turro, N. J. Modern Molecular Photochemistry; University Sciences Books: Sausalito, **1991.**

8 Atkins, P. W.; Friedman, R. S. Molecular Quantum Mechanics, 3rd ed.; Oxford University Press: New York, **1997.**

9 Griffiths, J. *Chem. Soc. Rev.* **1972,** *1*, 481–493.

10 Freiberg, S.; Lagugné-Labarthet, F.; Rochon, P.; Natansohn, A. *Macromolecules* **2003, 2680–2688.**

11 Rau, H. In Photochemistry and Photophysics; Rabek, J. K., Ed.; CRC Press: Boca Raton, FL, **1990; Vol.** *II*, Chapter 4. pp. 119–41.

12 Shin, D. M.; Schanze, K. S.; Whitten, D. G. J. *Am. Chem. Soc.* **1989,** *111*, 8494–8501.

13 Rivera, E.; Belletête, M.; Natansohn, A.; Durocher, G. *Can. J. Chem.* **2003,** *81*, 1076–1082.

14 Rivera, E.; Carreón-Castro, M. P.; Buendía, I.; Cedillo, G. *Dyes Pigments* **2006,** *68*, 217–226.

15 Rivera, E.; Carreón-Castro, M. P.; Rodriguez, L.; Cedillo, G.; Fomine, S.; Morales-Saavedra, O. G. *Dyes Pigments* **2007,** *74*, 396–403.

16 Rivera, E.; Carreón-Castro, M. P.; Salazar, R.; Huerta, G.; Becerril, C.; Rivera, L. *Polymer* **2007,** *48*, 3420–3428.

17 He, X. H.; Zhang, H. L.; Yan, D. L.; Wang, X. J. *Polym. Sci. Part A: Polym. Chem.* **2003,** *41*:2854–2864.

18 Tian, Y. Q.; Watanabe, K.; Kong, X. X.; Abe, J.; Iyoda, T. *Macromolecules* **2002,** *36*, 3739–3749.

19 Saito, M.; Shimomura, T.; Okumura, Y.; Ito, K.; Hayakawa, R. J. *Chem. Phys.* **2001,** *114*, 1–3.

20 Shimomura, T.; Funaki, T.; Ito, K. J. *Inclusion Phenom. Macroc. Chem.* **2002,** *44*, 275–278.

21 Zheng, P. J.; Wang, C.; Hu, X.; Tam, K. C.; Li, L. *Macromolecules* **2005,** *38*, 2859–2864.

22 Hu, X.; Zheng, P. J.; Zhao, X. Y.; Li, L.; Tam, K. C.; Gan, L. H. *Polymer* **2004,** *45*:6219–6225.

23 Takashima, Y.; Nakayama, T.; Miyauchi, M.; Kawaguchi, Y. *Chem. Lett.* **2004,** *33*, 890–891.

24 Ikeda, T.; Ooya, T.; Yui, N. *Polym. J.* **1999,** *31*, 658–663.

25 Tung, C. H.; Wu, L. Z.; Zhang, L. P.; Chen, B. *Acc. Chem. Res.* **2003,** *36*, 39–47.

26 Pojman, J. A.; Tran-Cong-Miyata, Q. Nonlinear Dynamics with Polymers: Fundamentals, Methods and Applications; Wiley-VCH: Weinheim, **2010.**

27 Chechilo, N. M.; Enikolopyan, N. S. *Dokl. Phys. Chem.* **1974,** *214*, 174–176.

28 Davtyan, S. P.; Zhirkov, P. V.; Vol'fson, S. A. *Russ. Chem. Rev.* **1984,** *53*, 150–163.

29 Mariani, A.; Bidali, S.; Cappelletti, P.; Caria, G.; Colella, A.; Brunetti, A.; Alzari, V. *e-Polymers* **2009,** *064*, 1–12.

30 Vicini, S.; Mariani, A.; Princi, E.; Bidali, S.; Pincin, S.; Fiori, S.; Pedemonte, E.; Brunetti, A. *Polym. Adv. Technol.* **2005,** *16*, 293–298.

31 Fiori, S.; Mariani, A.; Ricco, L.; Russo, S. *e-Polymers* **2002,** *029*, 1–10.

32 Fiori, S.; Mariani, A.; Bidali, S.; Malucelli, G. *e-Polymers* **2004,** *001*, 1–12.

33 Fiori, S.; Malucelli, G.; Mariani, A.; Ricco, L.; Casazza, E. *e-Polymers* **2002,** *057*, 1–10.

34 Caria, G.; Alzari, V.; Monticelli, O.; Nuvoli, D.; Kenny, J. M.; Mariani, A. J. *Polym. Sci. Part A: Polym. Chem.* **2009,** *47*, 1422–1428.

35 Gavini, E.; Mariani, A.; Rassu, G.; Bidali, S.; Spada, G.; Bonferoni, M. C.; Giunchedi, P. *Eur. Polym. J.* **2009,** *45*, 690–699.

36 Alzari, V.; Monticelli, O.; Nuvoli, D.; Kenny, J. M.; Mariani, A. *Biomacromolecules* **2009,** *10*, 2672–2677.

37 Scognamillo, S.; Alzari, V.; Nuvoli, D.; Mariani, A. J. *Polym. Sci. Part A: Polym. Chem.* **2010,** *48*, 2486–2490.

38 Mariani, A.; Bidali, S.; Caria, G.; Monticelli, O.; Russo, S.; Kenny, J. M. J. *Polym. Sci. Part A: Polym. Chem.* **2007,** *45*, 2204–2212.

39 Mariani, A.; Alzari, V.; Monticelli, O.; Pojman, J. A.; Caria, G. J. *Polym. Sci. Part A: Polym. Chem.* **2007,** *45*, 4514–4521.

40 Scognamillo, S.; Alzari, V.; Nuvoli, D.; Mariani, A. J. *Polym. Sci. Part A: Polym. Chem.* **2010,** *48*, 4721–4725.

41 Alzari, V.; Mariani, A.; Monticelli, O.; Valentini, L.; Nuvoli, D.; Piccinini, M.; Scognamillo, S.; Bittolo Bon, S.; Illescas, J. J. *Polym. Sci. Part A: Polym. Chem.* **2010,** *48*, 5375–5381.

42 Illescas, J.; Ramírez-Fuentes, Y. S.; Rivera, E.; Morales-Saavedra, O. G.; Rodríguez-Rosales, A. A.; Alzari, V.; Nuvoli, D.; Scognamillo, S.; Mariani, A. J. *Polym. Sci. Part A: Polym. Chem.* **2011,** *49*, 3291–3298.

43 Illescas, J.; Ramírez-Fuentes, Y. S.; Rivera, E.; Morales-Saavedra, O. G.; Rodríguez-Rosales, A. A.; Alzari, V.; Nuvoli, D.; Scognamillo, S.; Mariani, A. J. *Polym. Sci. Part A: Polym. Chem.* **2012,** *50*, 821–830.

44 Alzari, V.; Nuvoli, D.; Scognamillo, S.; Piccinini, M.; Gioffredi, E.; Malucelli, G.; Marceddu, S.; Sechi, M.; Sanna, V.; Mariani, A. J. *Mater. Chem.* **2011,** *21*, 8727–8733.

45 Hu, T.; Chen, S.; Tian, Y.; Chen, L.; Pojman, J. A. J. *Polym. Sci. Part A: Polym. Chem.* **2007,** *45*, 873–881.

46 Chen, S.; Tian, Y.; Chen, L.; Hu, T. *Chem. Mater.* **2006,** *18*, 2159–2163.

47 Cai, X.; Chen, S.; Chen, L. J. *Polym. Sci. Part A: Polym. Chem.* **2008,** *46*, 2177–2185.

48 Fang, Y.; Chen, L.; Wang, C. F.; Chen, S. J. *Polym. Sci. Part A: Polym. Chem.* **2010,** *48*, 2170–2177.

49 Chen, S.; Sui, J.; Chen, L.; Pojman, J. A. J. *Polym. Sci. Part A: Polym. Chem.* **2005,** *43*, 1670–1680.

50 Tu, J.; Chen, L.; Fang, Y.; Wang, C.; Chen, S. J. *Polym. Sci. Part A: Polym. Chem.* **2010,** *48*, 823–831.

51 Tu, J.; Zhou, J.; Wang, C.; Zhang, Q.; Chen, S. J. *Polym. Sci. Part A: Polym. Chem.* **2010,** *48*, 4005–4012.

52 Pojman, J. A.; Ilyashenko, V. M.; Khan, A. M. J. *Chem. Soc. Faraday Trans.* **1996,** *92*, 2825–2837.

53 Nagy, I. P.; Pojman, J. A. J. *Phys. Chem.* **1996,** *100*, 3299–3304.

54 Ilyashenko, V. M.; Pojman, J. A. *Chaos* **1998,** *8*, 285–289.

55 Pojman, J. A.; Masere, J.; Pettreto, E.; Rustici, M.; Volpert, V. *Chaos* **2002,** *12*, 56–65.

56 Mariani, A.; Fiori, S.; Chekanov, Y.; Pojman, J. A. *Macromolecules* **2001,** *34*, 6539–6541.

57 Pojman, J. A.; Chen, L. J. *Polym. Sci. Part A: Polym. Chem.* **2006,** *44*, 3018–3024.

58 Nason, C.; Pojman, J. A.; Hoyle, C. J. *Polym. Sci. Part A: Polym. Chem.* **2008,** *46*, 8091–8096.

59 Nason, C.; Roper, T.; Hoyle, C.; Pojman, J. A. *Macromolecules* **2005,** *38*, 5506–5512.

60 Fortenberry, D. I.; Pojman, J. A. J. *Polym. Sci. Part A: Polym. Chem.* **2000,** *38*, 1129–1135.

61 McFarland, B.; Popwell, S.; Pojman, J. A. *Macromolecules* **2006,** *39*, 53–63.

62 Pojman, J. A.; Elcan, W.; Khan, A. M.; Mathias, L. J. *Polym. Sci. Part A: Polym. Chem.* **1997,** *35*, 227–230.

63 Scognamillo, S.; Bounds, C.; Luger, M.; Mariani, A.; Pojman, J. A. J. *Polym. Sci. Part A: Polym. Chem.* **2010,** *48*, 2000–2005.

64 Viner, V. G.; Pojman, J. A.; Golovaty, D. *Phys. D: Nonlinear Phenom.* **2010,** *239*, 838–847.

65 Mariani, A.; Nuvoli, D.; Alzari, V.; Pini, M. *Macromolecules* **2008,** *41*, 5191–5196.

66 Rodríguez-Rosales, A. A.; Morales-Saavedra, O. G.; Román, C. J.; Ortega-Martínez, R. *Opt. Mat.* **2008,** *31*, 350–360.

67 Liu, X.; Guo, S.; Wang, H.; Hou, L. *Opt. Commun.* **2001,** *197*, 431–437.

68 Sheik-Bahae, M.; Said, A. A.; Van Stryland, E. W. *Opt. Lett.* **1989,** *14*, 955–957.

69 Sheik-Bahae, M.; Said, A. A.; Hagan, D. J.; Soileau, M. J.; Van Stryland, E. W. *Opt. Eng.* **1991,** *30/8*, 1228–1235.

70 Sheik-Bahae, M.; Said, A. A.; Wei, T. H.; Hagan, D. J.; Van Stryland, E. W. *IEEE J. Quantum Electron.* **1990,** *26*, 760–769.

71 Xia, T.; Hagan, D. J.; Sheik-Bahae, M.; Van Stryland, E. W. *Opt. Lett.* **1994,** *19*, 317–319.

72 Nonlinear Optics of Organic Molecules and Polymers; Nalwa, H. S.; Miyata S., Eds.; CRC Press: Boca Raton, FL, **1997.**

73 Natansohn, A.; Rochon, P.; Gosselin, J.; Xie, S. *Macromolecules* **1992,** *25*, 2268–2273.

74 Rochon, P.; Gosselin, J.; Natansohn, A.; Xie, S. *Appl. Phys. Lett.* **1992,** *60*, 4–5.

75 Masere, J.; Chekanov, Y.; Warren, J. R.; Stewart, F. D.; Al-Kaysi, R.; Rasmussen, J. K.; Pojman, J. A. J. *Polym. Sci. Part A: Polym. Chem.* **2000,** *38*, 3984–3990.